COMPUTER SIMULATION OF AlCoCuFeNi HIGH-ENTROPY ALLOY THIN FILM DEPOSITION AND CRYSTALLIZATION

O.I. Kushnerov*

Oles Honchar Dnipro National University, Dnipro, Ukraine
**e-mail: kushnrv@gmail.com*

The processes of deposition and crystallization of high-entropy AlCoCuFeNi alloy thin film on a substrate of silicon (100) are studied by classical molecular dynamics simulation. Total simulation time reaches 50 ns. The embedded atom model is used to describe the interaction among Al–Co–Cu–Ni–Fe. Interaction between the atoms of Al, Co, Cu, Fe, Ni, and the Si substrate is described using the Lennard–Jones potential, and the interaction between the silicon atoms was modeled using the Stillinger–Weber potential. It is found that at the first stage of deposition small clusters are formed and the process of crystallization starts after ~ 5 ns of simulation, at the characteristic sizes of clusters of about 2 nm. At the end of the simulation, after the 50 ns of modeling, the simulated film contains a face-centered cubic phase, a body-centered cubic phase, a hexagonal close-packed phase, and an amorphous phase. An analysis of the radial distribution of atoms makes it possible to determine the distances between the nearest neighbors and estimate the lattice parameters of these phases.

Keywords: high-entropy alloy, molecular dynamics, structure, thin film.

Received 11.09.2022; Received in revised form 18.10.2021; Accepted 15.11.2022

1. Introduction

High-entropy alloys (HEAs) are a relatively new class of metallic materials developed by Yeh et al. in 2004. Such alloys usually contain from 5 to 13 basic elements in equiatomic or close to equiatomic concentrations (from 5 to 35%). Due to the high mixing entropy, multicomponent HEAs typically consist of simple solid solutions with face-centered cubic (FCC) or body-centered cubic (BCC) lattices. Many HEAs possess unique properties, such as wear-resistance, resistance to corrosion and oxidation, radiation resistance, high hardness, and strength [1–5]. Thus, the HEAs may find use as materials for nuclear reactors applications, medicine, electronics devices, mechanical equipment, rocket casings, engines etc. The majority of HEAs were investigated in the as-quenched or homogenized state, whereas much less attention was paid to the study of thin films of HEAs. However, due to the very high cooling rates required to avoid the formation of complex crystallized phases and freeze the low-ordered structures, HEA is sometimes difficult to synthesize as bulk materials. The study of the growth characteristics of complex multi-element HEA films is an important topic of research considering that thin films as well as other nano-objects can be used in various fields of technology [6, 7]. Some papers [8, 9] have been devoted to the study of thin film growth processes of one of the earliest and best-studied HEA of the AlCoCrCuFeNi system. However, a five-element AlCoCuFeNi HEA was developed later. This alloy does not contain Cr, which is commonly used in HEAs, and helps to improve their performance, but significantly increases the cost of the alloy. In this work, the processes of deposition and growth of thin films of AlCoCuFeNi HEA on the surface of a monocrystalline silicon substrate are investigated by classical molecular dynamics (MD) simulation.

2. Simulation model and methods

Classical MD simulation studies of deposition and growth of thin films of AlCoCuFeNi HEA were performed using Large Scale Atomic/Molecular Massively Parallel Simulator (LAMMPS, Sandia National Laboratory, USA) [10]. Visualization of snapshots and the coordination analysis were done using open visualization tool software OVITO [11]. A three-dimensional cell with periodic boundary conditions only in two horizontal directions x and y was used. The free boundary condition was used in the vertical *z*-direction to ensure surface growth. The monocrystalline Si (100) substrate was $10 \times 10 \times 2.2$ nm. To prevent substrate

displacement due to the impact of adatoms on the upper surface of the substrate, the positions of several lower atomic planes were fixed. The intermediate region of the substrate above the stationary atomic planes was controlled by a Berendsen thermostat and maintained at a temperature of 300 K which is similar to the experimental temperature mode to ensure isothermal growth conditions. The atoms of the upper layers of the substrate were not subjected to thermostating and were able to move freely under the impact of the deposited atoms. The 5 atoms of metals Al, Co, Cu, Fe, and Ni in the equimolar ratio were directed to the substrate every 10 ps, this led to the atomic flux density of $5 \cdot 10^{23}$ atom/(cm^2·s). The rate of 0.5 atom/ps was carefully chosen to allow sufficient time for thermal relaxation with a Berendsen thermostat (i.e. the substrate energy relaxation after collision). It should be borne in mind that the flux of atoms in the MD simulation is much more than in the experiment, but the obtained data on morphology, structure, and adhesion coefficient are quite adequate [9]. The velocities of the deposited atoms corresponded to the mean kinetic energy of 0.1 eV. The initial positions of the deposited atoms were chosen randomly in the $\{x, y\}$ plane above substrate so that they were outside the range of the potential that described the interaction in the *z*-direction. All of Al, Co, Cu, Fe, and Ni atoms were deposited from an initial position 15.7–16 nm above the substrate.

The simulation was carried out using the embedded atom model (EAM) [12] to describe the interaction among Al–Co–Cu–Ni–Fe. EAM potentials include empirical formulas that simulate material characteristics such as surface energies, lattice constants, and the heat of solution. The EAM potential is based on the ideas of density functional theory, which generally state that the energy of a solid is a unique function of electron density.

In the present research, the EAM potential developed by Zhou et al. [13] was used. The interaction between the atoms of Al, Co, Cu, Fe, Ni, and the Si substrate was modeled using the Lennard–Jones potential with the parameters summarized in [8, 9], and the interaction between the silicon atoms was described using the Stillinger–Weber potential [14].

3. Results and discussion

During simulation 25000 atoms were deposited to the substrate, which corresponded to the nominal equiatomic AlCoCuFeNi composition, but some of them were escaping the surface and the resulting film contained only 24433 atoms. So, the sticking coefficient was ≈ 0.98. The composition of the simulated HEA film and the target composition is shown in Table 1.

Table 1

The element composition in a simulated thin film of AlCoCuFeNi HEA

Number of atoms in	Al	Co	Cu	Fe	Ni	Total
nominal composition	5000	5000	5000	5000	5000	25000
resulting film	4909	4877	4865	4889	4893	24433

Thus, the final composition of the simulated AlCoCuFeNi film was quite close to equiatomic.

According to the results of the simulation, it was found that at the initial stages of growth (0 – 2 ns) the film represented an islet-like structure formed by small clusters (Fig. 1). Later, the growth of the islands and the formation of continuous coating began. Due to the limited number of deposited atoms, it was impossible to obtain a completely continuous film even after 50 ns of simulation time. The maximum thickness of the film had reached 4.3 nm. Following the results of common neighbor analysis (CNA), the

process of crystallization started after ~ 5 ns of simulation, at the characteristic sizes of islands (clusters) of about 2 nm.

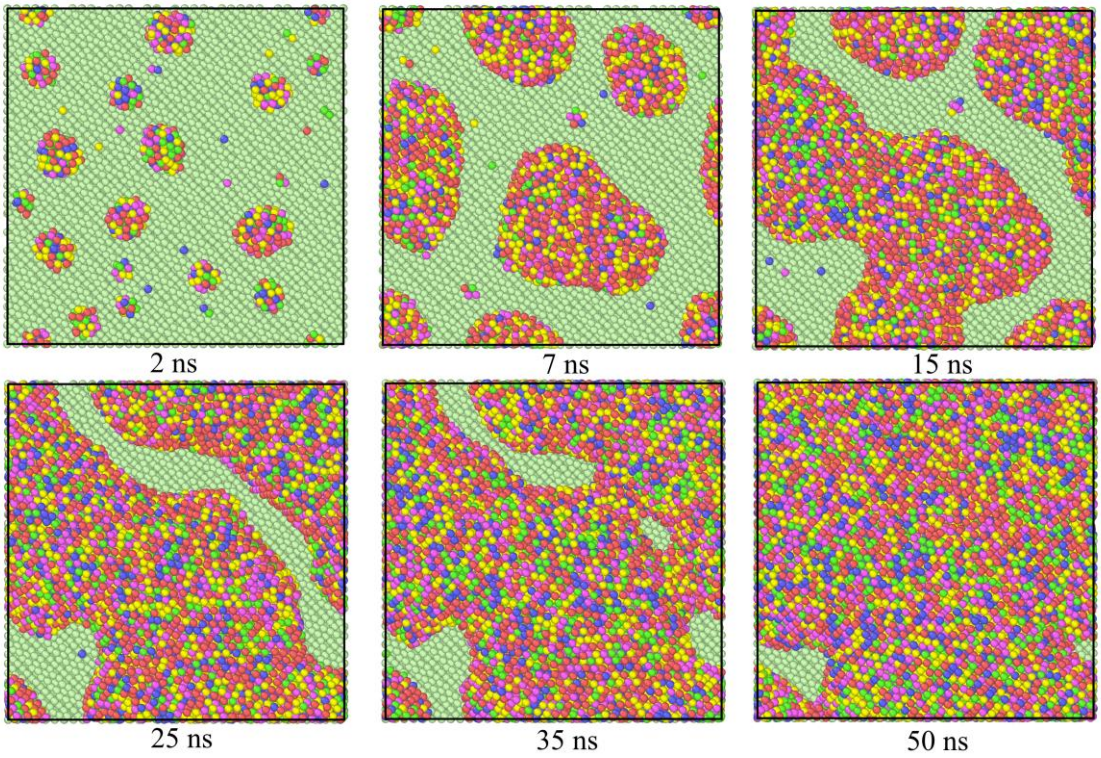

Fig. 1. Snapshots of AlCoCuFeNi thin film deposited on Si substrate at different times (top view): ● – Al, ● – Co, ● – Cu, ● – Fe, ● – Ni.

At the end of the simulation, after the 50 ns of modeling, the simulated film contains a face-centered cubic (FCC) phase (content 20.5 %), a body-centered cubic (BCC) phase (content 13.2%), a hexagonal close-packed (HCP) phase (content 39.7%) (Fig. 2) and an indefinite phase (content 26.6%), which, according to the analysis of the radial distribution of atoms (RDF), has an amorphous structure.

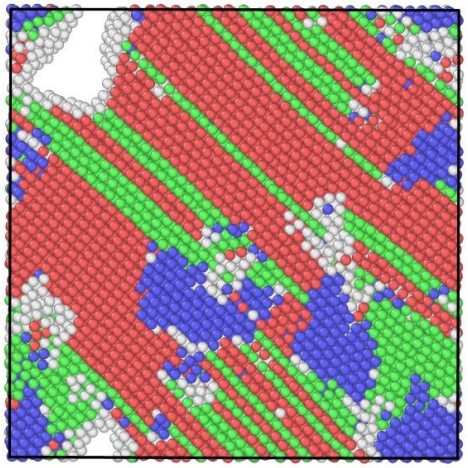

Fig. 2. Snapshot of AlCoCuFeNi thin film sliced along the substrate plane (top view). Atoms are colored according to CNA analysis results: ● – FCC, ● – BCC, ● – HCP, ● – amorphous phase.

It should be noted that in bulk AlCoCuFeNi alloy only the presence of FCC and BCC phases was recorded [15], but at the same time in melt-spun films, the formation of the nanotwin structure and stacking faults in the FCC phase was noted [16]. Thus, the specific features of the distribution of the HCP phase atoms (Fig. 2) lead to the conclusion that this phase must be formed mainly of extrinsic (two HCP layers with an FCC layer between them) and intrinsic (two or more adjacent HCP layers) stacking faults in the lattice of the FCC phase. There are also twin boundaries between the FCC twins (a single layer composed of HCP atoms). The presence of such structures was previously noted during the molecular dynamics study of nanoparticles and nanowires of the AlCoCuFeNi alloy [17, 18]. As for the amorphous phase, its formation is explained by the high cooling rate that occurs during film deposition, at which some of the atoms do not have time to rearrange and form a crystalline phase. In the context of the present simulation, this concerns mainly atomic layers located near the film surface, while crystallization processes take place in deeper layers.

It is well known from the literature, that there are two main criteria by which the high-entropy alloys are usually characterized. This is the entropy of mixing ΔS_{mix} and the enthalpy of mixing ΔH_{mix}. However, to predict the phase composition of HEAs, some additional parameters were proposed [1, 2]. These parameters include the valence electron concentration (VEC) and the thermodynamic parameter Ω, which takes into account the melting temperature, mixing entropy, and the mixing enthalpy. The important parameter is an atomic-size difference between alloy components which is denoted as δ. Using the data from [19 ,20] we calculated ΔS_{mix}, ΔH_{mix}, δ, VEC, and Ω for the AlCoCuFeNi HEA (Table 2).

Table 2

Electronic, thermodynamic, and the atomic-size parameters of the AlCoCuFeNi HEA

ΔS_{mix}, J/(mol·K)	ΔH_{mix}, kJ/mol	Ω	VEC	δ
13.37	-5.28	3.847	8.2	5.323

According to [1, 2] the HEA alloys, for which Ω≥1.1 and δ≤6.6, can form solid solutions without intermetallic compounds. However, simple (not ordered) solid solutions are formed if -15 kJ/mol < ΔH_{mix} < 5 kJ/mol. The other useful parameter is VEC, which has been proven suitable in determining the phase stability of high-entropy alloys. As pointed in [21] at VEC ≥8.0, the sole FCC phase is expected in the alloy; at 6.87 ≤ VEC < 8.0, mixed FCC and BCC phases will coexist, and the sole BCC phase is expected at VEC < 6.87. Thus, the simulation results, as well as the experimental results, generally confirm the validity of the above criteria, except for the VEC parameter. But, if the value of VEC is close to the boundary values, predictions of the phase compositions sometimes do not work [5].

Fig. 3 presents the total RDF curves after 50 ns of simulation time. RDF patterns are obtained both for the film as a whole and for individual phases separated by CNA analysis. It is clearly visible that the RDF form of an indefinite phase is intermediate between liquid and crystal, indicating an amorphous structure. The peaks on the RDF curves represent the successive distances between neighbors for different phases in the simulated film. So, from the RDF pattern for the whole film these distances are: 1-st neighbor – 0.2575 nm, 2-nd neighbor – 0.3725 nm, 3-rd neighbor – 0.4525 nm, 4-th neighbor – 0.4925 nm. Determining the distances between the nearest neighbors for the BCC and FCC lattices made it possible to estimate the lattice parameters for these phases. Table 3 shows the comparison between estimated parameters of the BCC and FCC lattices from the present MD simulation and the experimental results.

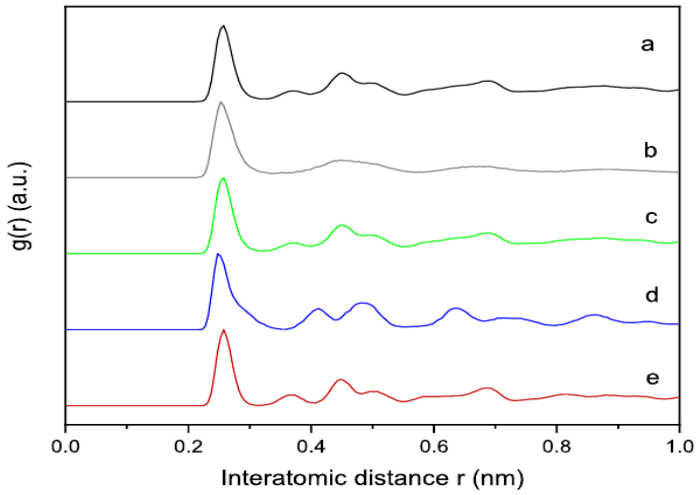

Fig. 3. The RDF curves of AlCoCuFeNi thin film: a – the whole film, b – amorphous phase, c – FCC phase, d – BCC phase, e – HCP phase.

Table 3

Calculated and experimental lattice parameters for AlCoCuFeNi HEA

Lattice parameter *a*, nm	Experiment, bulk alloy	Experiment, melt-spun ribbon	Calculated
BCC phase	0.2878	0.2872	0.2895
FCC phase	0.3624	0.3618	0.3670

As can be seen from Table 3, the calculated lattice parameters are in a good agreement with the experimental results, taking into account that the estimated average film temperature after 50 ns simulation was above the room temperature and was ≈350 K.

4. Conclusions

Molecular dynamics simulation was performed to describe the processes of growth and crystallization of thin AlCoCuFeNi HEA films. The structural characteristics and phase composition of films were examined utilizing CNA and RDF. According to simulation results, the growth of AlCoCuFeNi films occurs via the formation of three-dimensional adatom clusters or islands with subsequent coarsening and coalescence. The estimated lattice parameters of the BCC and FCC phases are in a good agreement with the lattice parameters of AlCoCuFeNi alloy obtained from the experiment.

References

1. High entropy alloys. Innovations, advances, and applications / T.S. Srivatsan, M. Gupta. – Boca Raton : CRC Press, 2020.–758 p.

2. High-entropy alloys. 2nd edition / B.S. Murty, J.W. Yeh, S. Ranganathan, P.P. Bhattacharjee. – Elsevier Science Publishing Co Inc, 2019. – 363 p.

3. **Miracle, D.B.** A critical review of high entropy alloys and related concepts/ D.B. Miracle, O.N. Senkov // Acta Materialia. – 2017. – Vol. 122. – P. 448–511.

4. **Kushnerov, O.I.** Structure and physical properties of cast and splat-quenched CoCr0.8Cu0.64FeNi high entropy alloy / O.I. Kushnerov, V.F. Bashev // East European Journal of Physics. – 2021. – No. 3. –P. 43–48.

5. **Kushnerov, O.I.** Structure and properties of nanostructured metallic glass of the Fe–B–Co–Nb–Ni–Si high-entropy alloy system / O.I. Kushnerov, V.F. Bashev, S.I. Ryabtsev // Springer Proceedings in Physics, –2021. – P. 557–567.

6. **Gulivets, A.N.** Multilayer compound Co-P films with controlled magnetic properties / A.N. Gulivets, V.A. Zabludovsky, E.P. Shtapenko, A.I. Kushnerev, M.P.

Dergachov, A.S. Baskevich // Transactions of the IMF. – 2002. – Vol. 80, No. 5. – P. 154–156.

7. **Vorovsky, V.Y.** Preparation of zinc oxide nanopowders doped with manganese, which have ferromagnetic properties at room temperature / V.Y. Vorovsky, A.V. Kovalenko, A.I. Kushneryov, O.V. Khmelenko // Functional Materials. – 2018. – Vol. 25, No. 1. – P. 61–66.

8. **Xie, L.** Molecular dynamics simulation of Al–Co–Cr–Cu–Fe–Ni high entropy alloy thin film growth / L. Xie, P. Brault, A. Thomann, X. Yang, Y. Zhang, G. Shang // Intermetallics. – 2016. – Vol. 68. – P. 78–86.

9. **Xie, L**. Molecular dynamics simulations of clusters and thin film growth in the context of plasma sputtering deposition / L. Xie, P. Brault, J. Bauchire, A. Thomann, L. Bedra // Journal of Physics D: Applied Physics. – 2014. – Vol. 47, No. 22. – P. 224004.

10. **Thompson, A.P.** LAMMPS – a flexible simulation tool for particle-based materials modeling at the atomic, meso, and continuum scales / A.P. Thompson, H.M. Aktulga, R. Berger, D.S. Bolintineanu, W.M. Brown, P.S. Crozier, P.J. in 't Veld, A. Kohlmeyer, S.G. Moore, T.D. Nguyen, R. Shan, M. J. Stevens, J. Tranchida, C. Trott, S. J. Plimpton // Computer Physics Communications. – 2022. – Vol. 271. – P. 108171.

11. **Stukowski, A.** Visualization and analysis of atomistic simulation data with OVITO–the open visualization tool / A. Stukowski // Modelling and Simulation in Materials Science and Engineering. – 2010. – Vol. 18, No. 1. – P. 015012.

12. **Daw, M.S.** The embedded–atom method: a review of theory and applications / M.S. Daw, S.M. Foiles, M.I. Baskes // Materials Science Reports. – 1993. – Vol. 9, No. 7–8. – P. 251–310.

13. **Zhou, X.W.** Misfit–energy–increasing dislocations in vapor-deposited CoFe/NiFe multilayers / X.W. Zhou, R.A. Johnson, H.N.G. Wadley // Physical Review B. – 2004. – Vol. 69, No. 14. – P. 144113.

14. **Stillinger, F.H.** Computer simulation of local order in condensed phases of silicon / F.H. Stillinger, T.A. Weber // Physical Review B. – 1985. – Vol. 31, No. 8. – P. 5262–5271.

15. **Liu, C.** Composition and phase structure dependence of mechanical and magnetic properties for $AlCoCuFeNi_x$ high entropy alloys / C. Liu, W. Peng, C. S. Jiang, H. Guo, J. Tao, X. Deng, Z. Chen // Journal of Materials Science & Technology. – 2019. – Vol. 35, No. 6. – P. 1175–1183.

16. **Yu, P.F.** Nanotwin's formation and growth in an AlCoCuFeNi high–entropy alloy / P.F. Yu, H. Cheng, L.J. Zhang, H. Zhang, M.Z. Ma, G. Li, P.K. Liaw, R.P. Liu // Scripta Materialia. – 2016. – Vol. 114. – P. 31–34.

17. **Kushnerov, O.I.** AlCoCuFeNi high-entropy alloy nanoparticle melting and solidification: a classical molecular dynamics simulation study /O.I. Kushnerov // Journal of Physics and Electronics. – 2019. – Vol. 27, No. 1. – P. 41–46.

18. **Kushnerov, O.I.** Molecular dynamics simulation of the solidification of AlCoCuFeNi high-entropy alloy nanowire / O. I. Kushnerov // Journal of Physics and Electronics. – 2019. – Vol. 27, No. 2. – P. 61–64.

19. **Takeuchi, A.** Classification of bulk metallic glasses by atomic size difference, heat of mixing and period of constituent elements and its application to characterization of the main alloying element/A. Takeuchi, A. Inoue// Materials Transactions.–2005. – V. 46. – P. 2817–2829.

20. **Li, W.K.** Advanced Structural Inorganic Chemistry/ W.K. Li, G.D. Zhou, T C. W. Mak. –New York: Oxford University Press, 2008. – 688 p.

21. **Guo, S.** Effect of valence electron concentration on stability of fcc or bcc phase in high entropy alloys / S. Guo, C. Ng, J. Lu, C.T. Liu // Journal of Applied Physics. – 2011. – Vol. 109, No. 10. – P. 103505.